Supplementary Information

Complexation of heavy metal cations with imidazolium ionic liquids lowers their reduction energy: implications for electrochemical separations

Shuai Tan,[a] Difan Zhang,[a] Ying Chen,[a] Benjamin A. Helfrecht,[a] Eric T. Baxter,[a] Wenjin Cao,[a] Xue-Bin Wang,[a] Manh-Thuong Nguyen,[a] Grant E. Johnson,[a*] and Venkateshkumar Prabhakaran[a*]*

[1]Physical and Computational Sciences Directorate, Pacific Northwest National Laboratory, Richland, Washington 99354, United States

*venky@pnnl.gov

*grant.johnson@pnnl.gov

*manhthuong.nguyen@pnnl.gov

***Operando* Raman Spectroscopy**

An aqueous solution of 1 M EMIMCl + 10 mM $PbCl_2$ was filled into a glass NMR tube (5 mm diameter, Wilmad® NMR tubes, Sigma Aldrich), sealed, and mounted on an aluminum sample holder with a built-in temperature control system. Raman spectroscopy measurements were performed using an in-house spectrometer equipped with a 633 nm excitation laser and a charge-coupled device (CCD) detection system (Andor, Shamrock 303i and iDus 416). The objective lens of the Raman microscope was placed at the curved edge of the NMR tube and a laser beam with an intensity of 2 – 3 mW was focused on the sample. The presented Raman data is spatially (10 spectra in an area of 1 x 1 mm^2) and temporally (integration time of 360 sec/spectra) averaged to ensure sample integrity throughout the measurements. Raman spectra were collected as a function of temperature after the set temperature was reached for 1 hour. The resolution of Raman spectra is 2 cm^{-1}

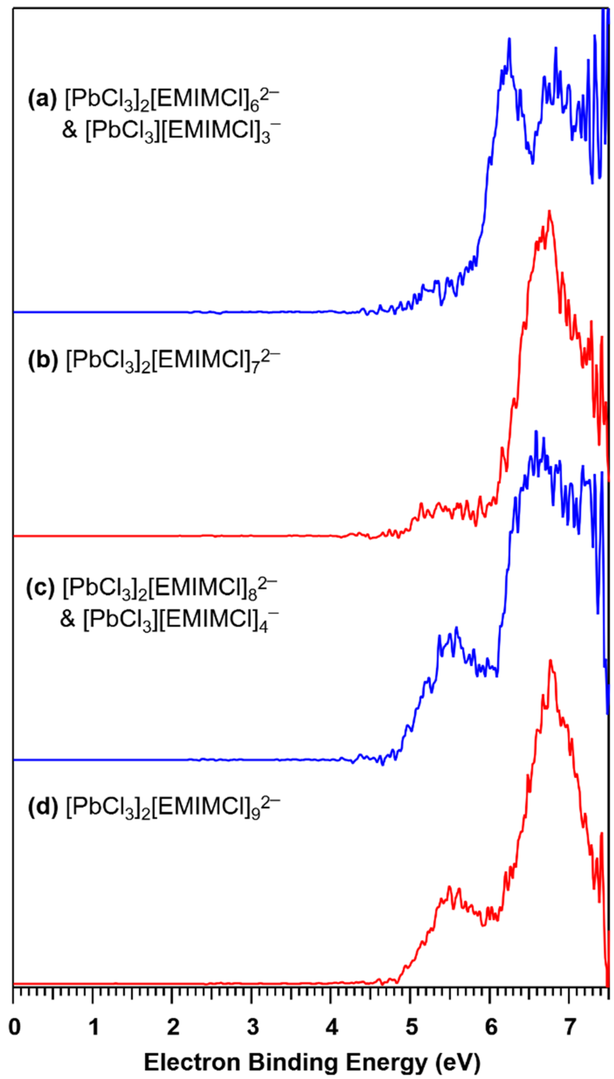

Figure S1. NIPES spectra of gas-phase doubly charged $[PbCl_3]_2[EMIMCl]_6^{2-}$ /$[PbCl_3][EMIMCl]_3^{-}$ (a), $[PbCl_3]_2[EMIMCl]_7^{2-}$ (b), $[PbCl_3]_2[EMIMCl]_8^{2-}$/$[PbCl_3][EMIMCl]_4^{-}$ (c), and $[PbCl_3]_2[EMIMCl]_9^{2-}$ (d) complexes. Note the *m/z* degenerate singly and doubly charged species.

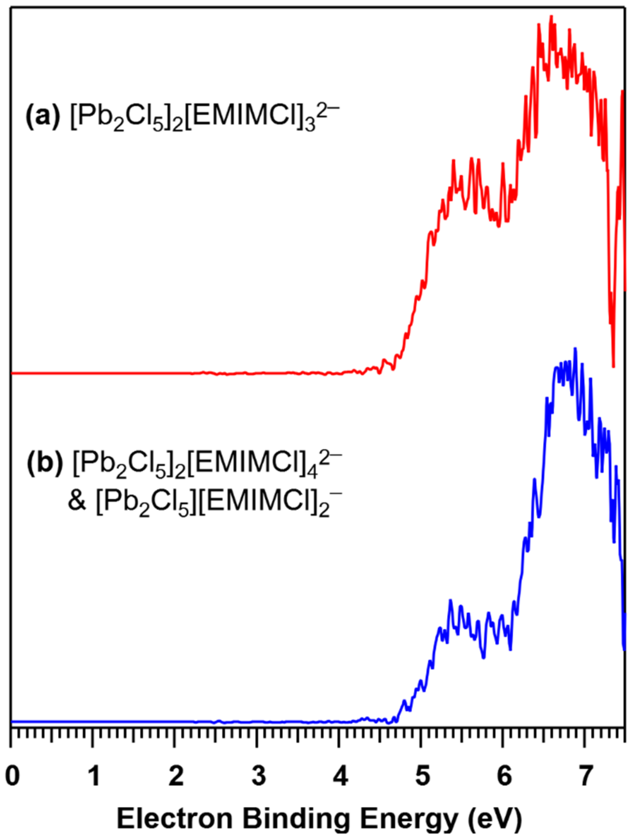

Figure S2. NIPES spectra of gas-phase doubly charged $[Pb_2Cl_5]_2[EMIMCl]_3^{2-}$ (a) and $[Pb_2Cl_5]_2[EMIMCl]_4^{2-}$/$[Pb_2Cl_5][EMIMCl]_2^{-}$ (b) complexes. Note the *m/z* degenerate singly and doubly charged species.

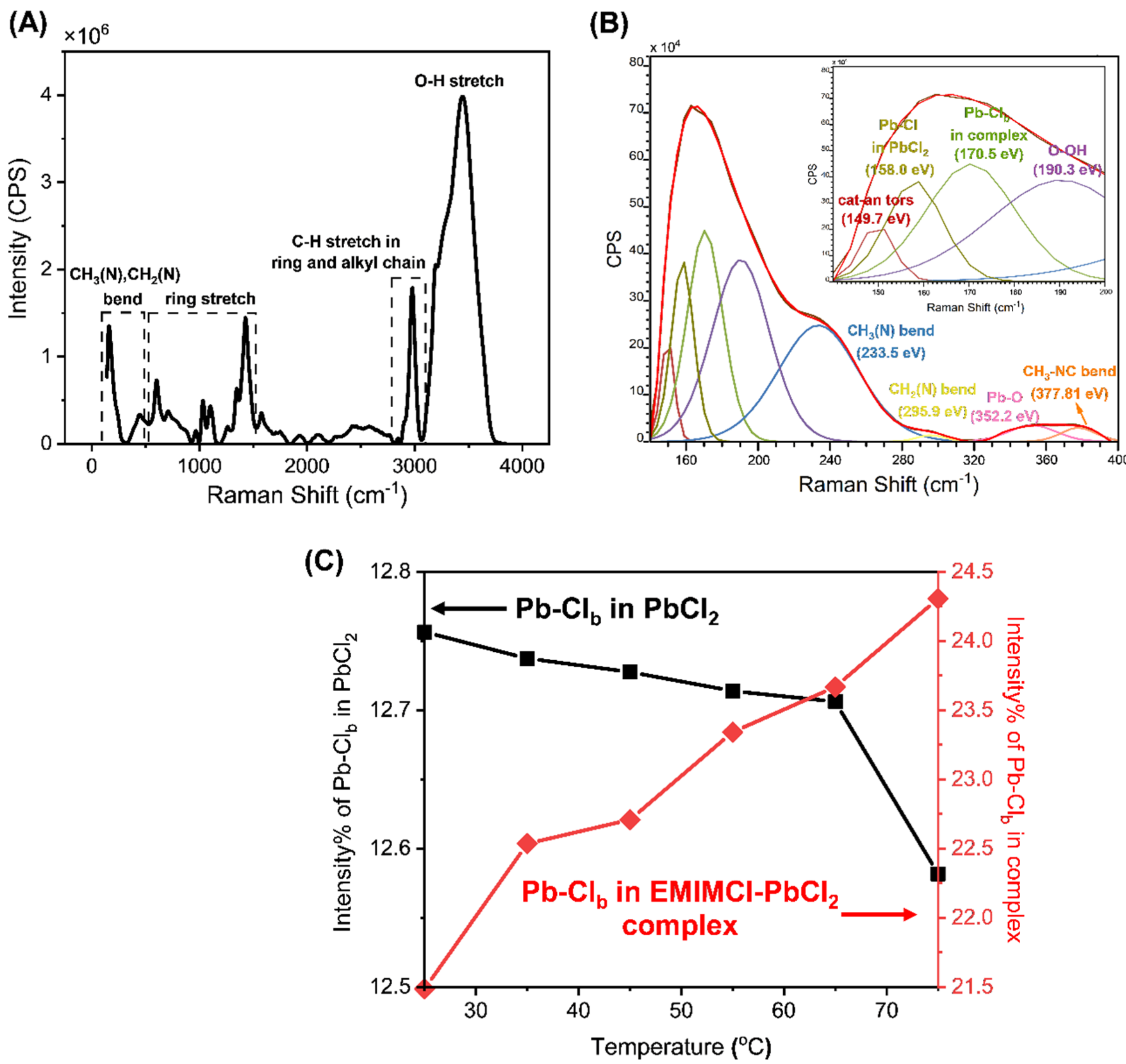

Figure S3. (A) Raman spectra in the range of 140 – 4000 cm^{-1} and (B) 140 – 400 cm^{-1} with deconvoluted fitting for the 1 M EMIMCl + 10 mM $PbCl_2$ aqueous solution. The inset of (B) is the spectrum between 140 – 200 cm^{-1}. (C) Change in the percent intensity of the Pb-Cl peak in $PbCl_2$ and Pb-Cl_b in the EMIMCl-$PbCl_2$ complex as a function of temperature.

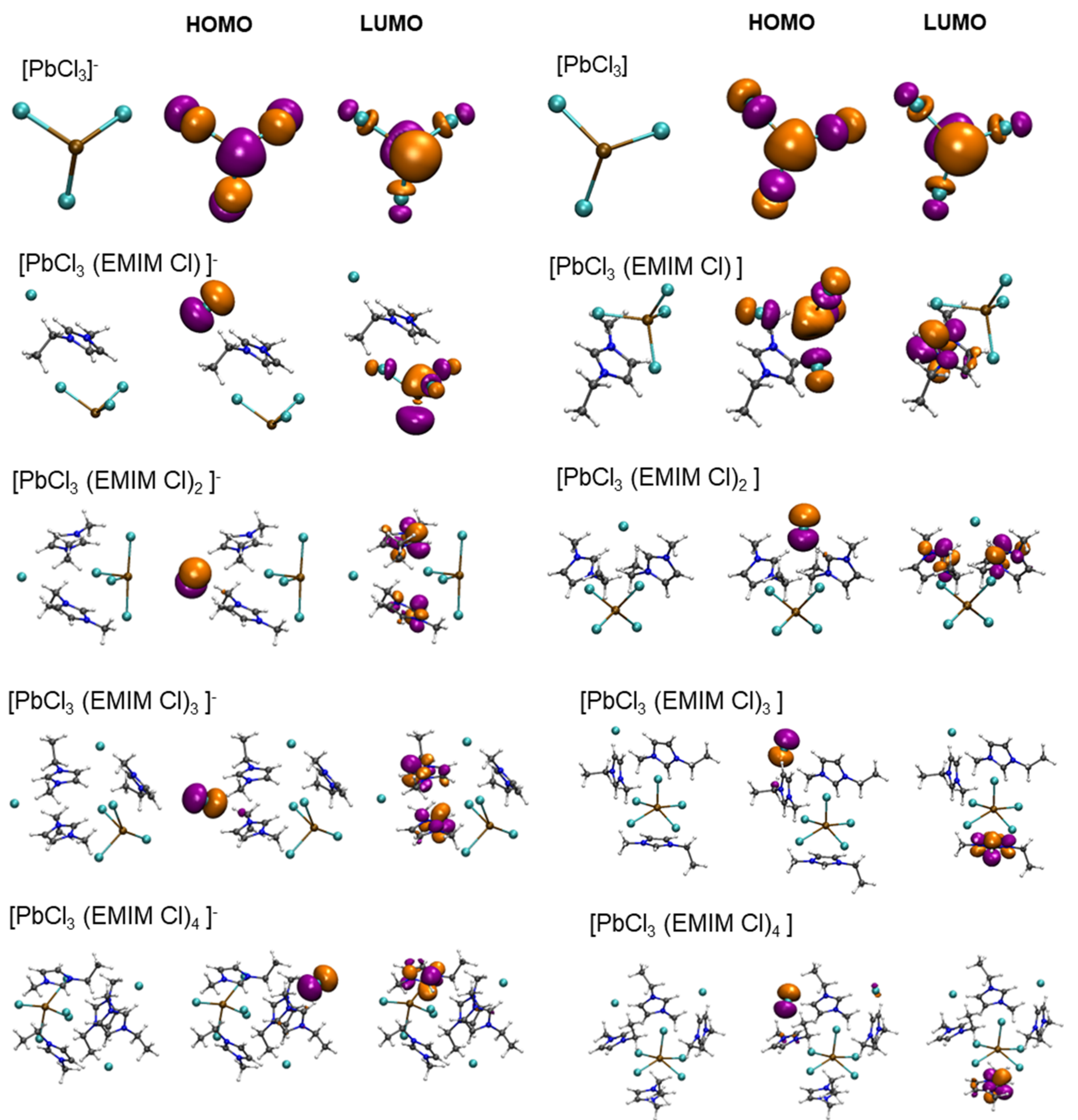

Figure S4. Visualization of the calculated HOMO and LUMO for gas phase $PbCl_3^-$ clusters with EMIMCl.

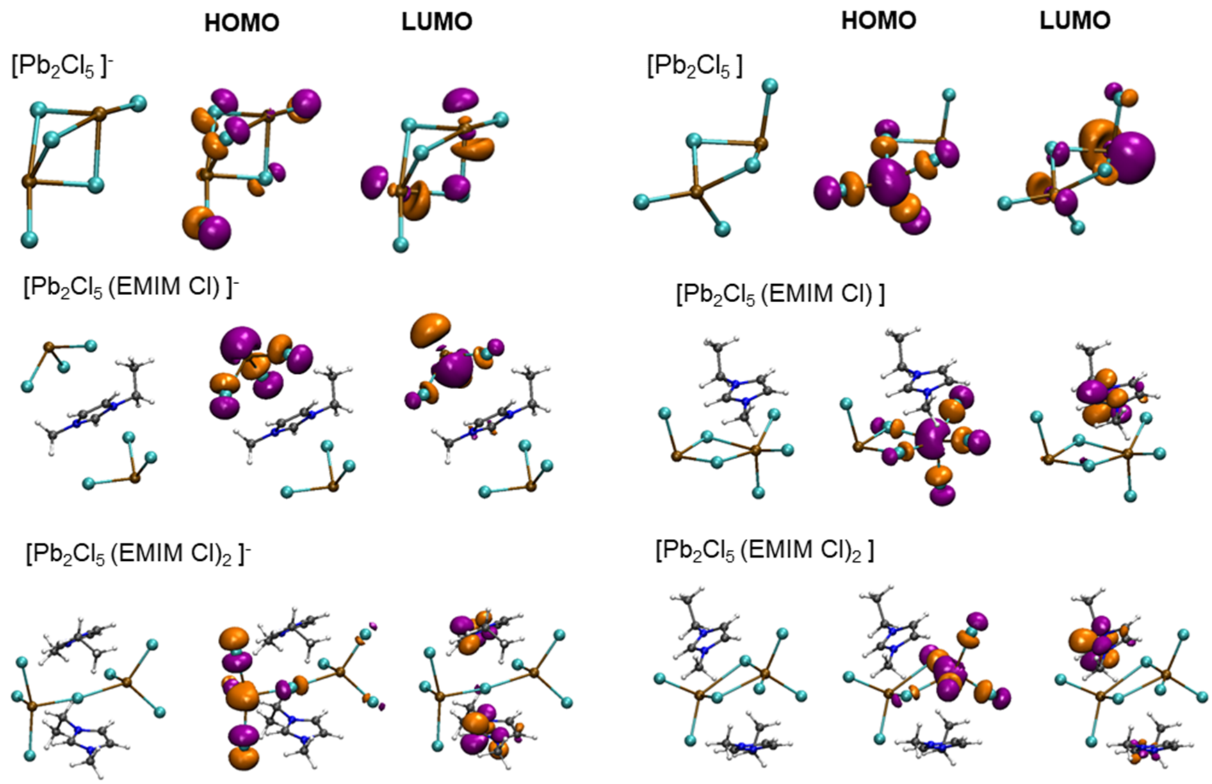

Figure S5. Visualization of the calculated HOMO and LUMO for gas phase $Pb_2Cl_5^-$ clusters with EMIMCl.

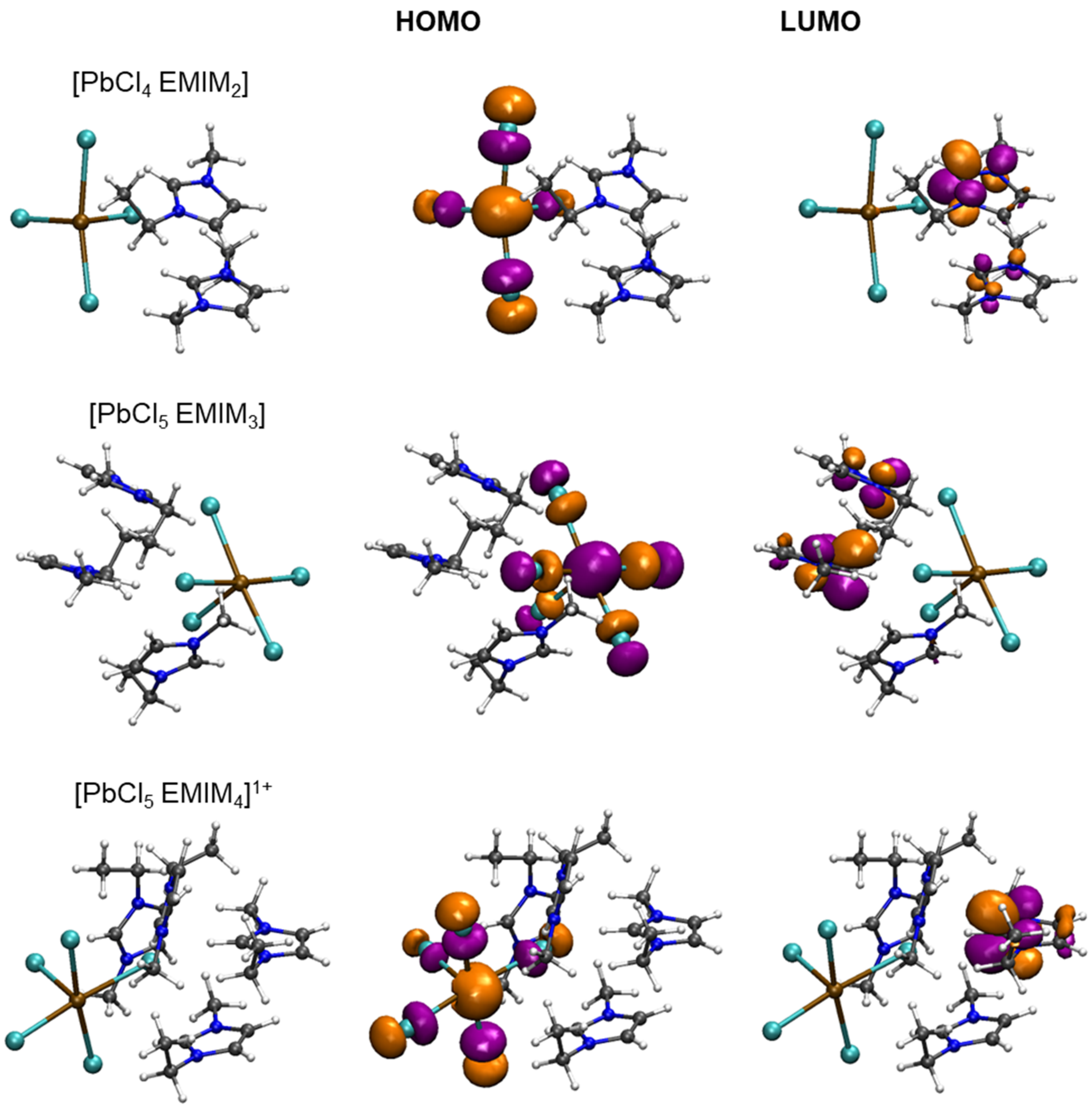

Figure S6. Visualization of the calculated HOMO and LUMO for aqueous phase Pb-Cl clusters with $EMIM^+$ cations identified by experimental NMR shifts.

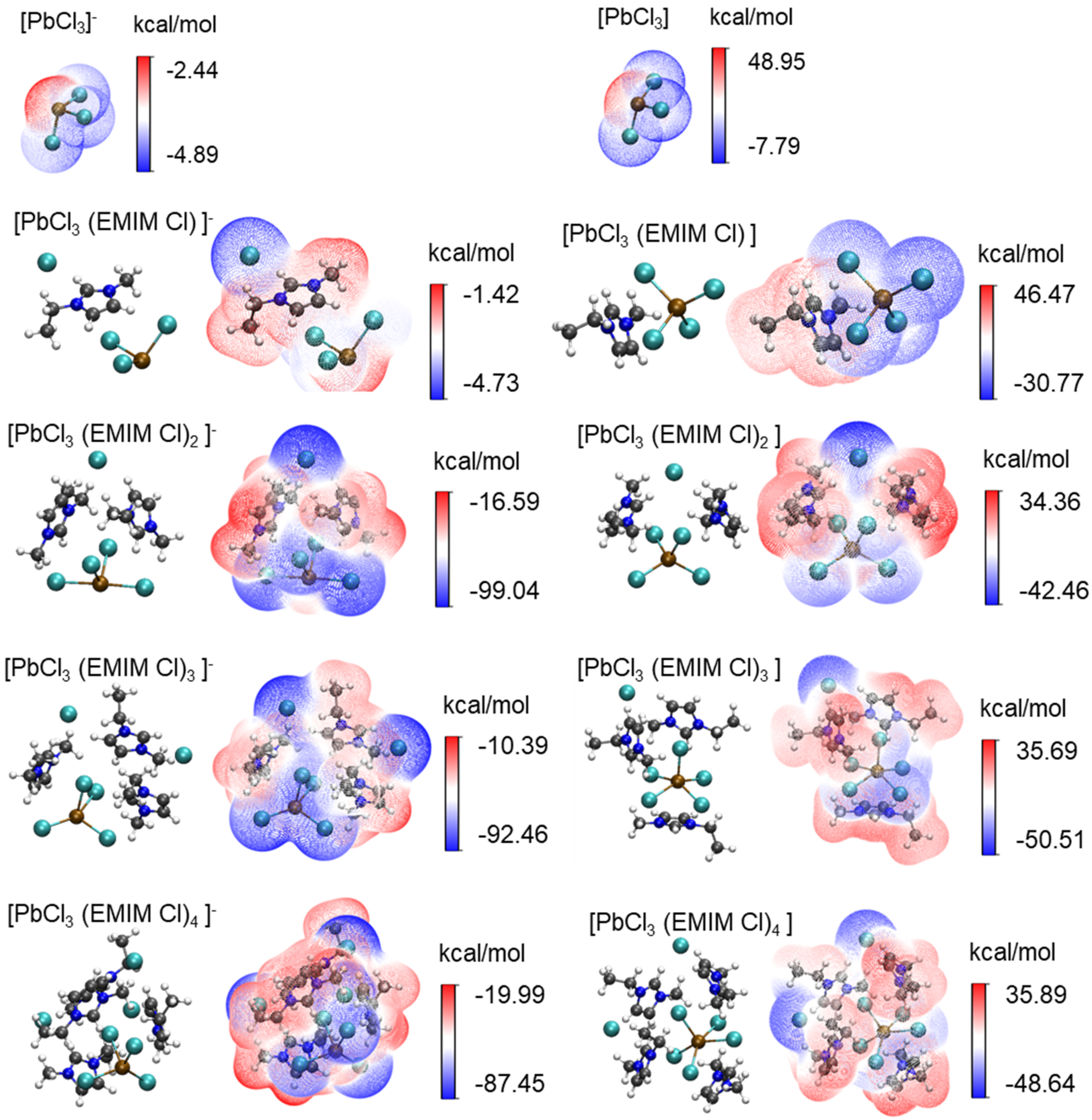

Figure S7. Visualization of the calculated ESP for gas phase $PbCl_3^-$ clusters with EMIMCl.

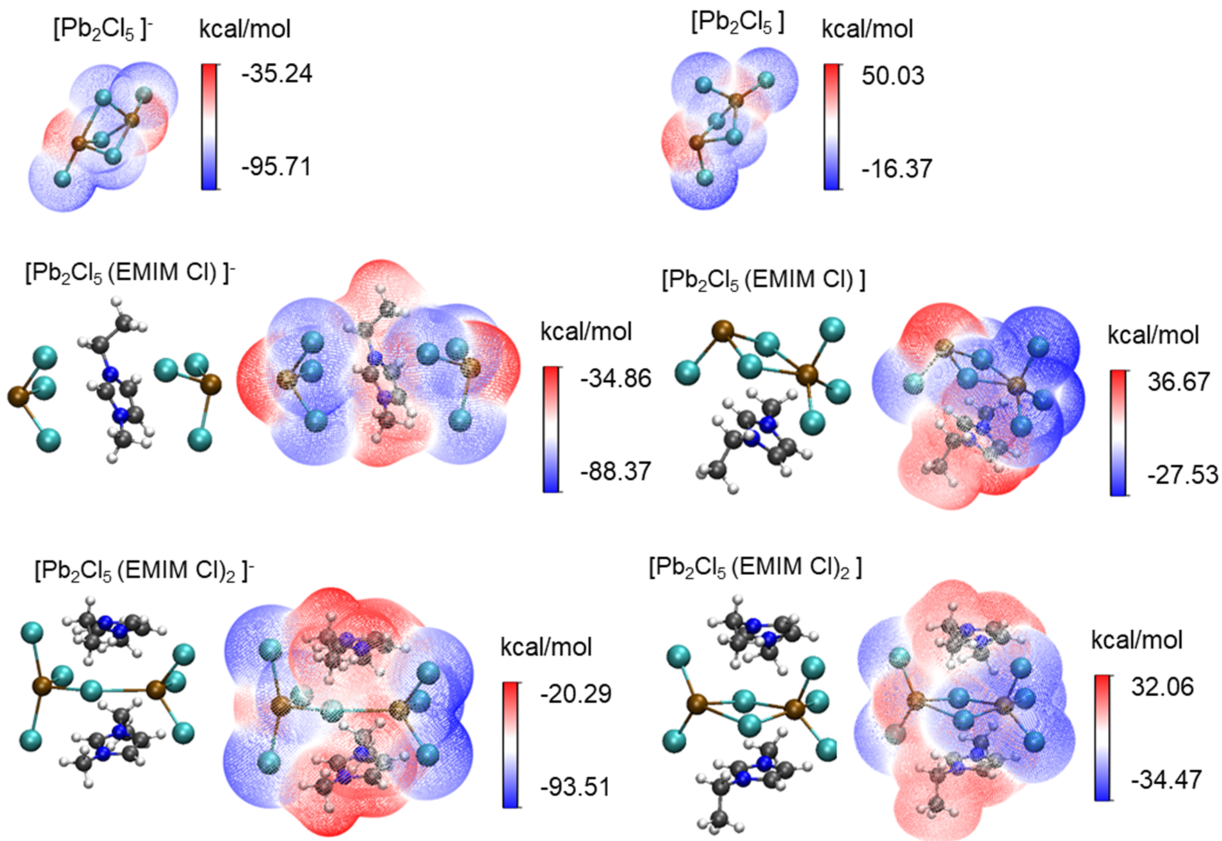

Figure S8. Visualization of the calculated ESP for gas phase $Pb_2Cl_5^-$ clusters with EMIMCl.

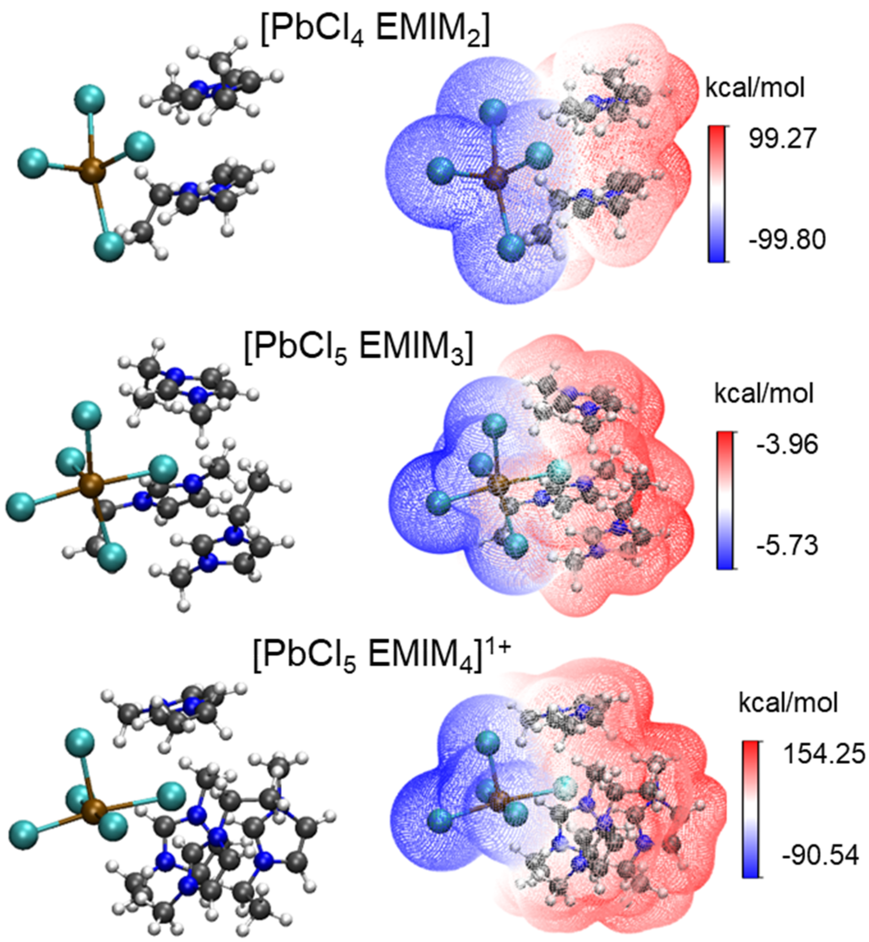

Figure S9. Visualization of the calculated ESP for aqueous phase $PbCl_{4-5}$ clusters with $EMIM^+$ cations identified by experimental NMR shifts.

Table S1. Experimentally measured ADE and VDE values (in eV) of the doubly charged $[PbCl_3]_n[EMIMCl]_x^{n-}$ and $[Pb_2Cl_5]_n[EMIMCl]_x^{n-}$ complexes.

n, x	**ADE**	**VDE**
	expt.[a]	expt.
	$[PbCl_3]_n[EMIMCl]_x^{n-}$	
2, 6	4.9	5.4
2, 7	4.9	5.4
2, 8	4.9	5.5
2, 9	4.9	5.5
	$[Pb_2Cl_5]_n[EMIMCl]_x^{n-}$	
2, 3	4.8	5.5
2, 4	4.9	5.4

[a]The experimental ADE represents an estimate of its upper limit.

Table S2. NMR ^1H T_1 and T_2 values of the two solutions containing EMIMCl and the difference in T_1 and T_2 values.

	KCl + EMIMCl		$PbCl_2$ + KCl + EMIMCl		Difference	
	^1H T_1 (s)	^1H T_2 (s)	^1H T_1 (s)	^1H T_2 (s)	T_1 (%)	T_2 (%)
H1	8.2	0.27	8.6	0.31	5	15
H2	11.4	0.59	11.1	0.33	-3	-44
H3	10.9	0.85	10.6	0.78	-3	-8
H4	5.5	0.72	5.2	0.71	-5	-1
H5	4.9	2.51	4.7	2.52	-4	0
H6	5.5	1.43	5.2	1.39	-5	-3

Table S3. Diffusion coefficients of H_2O and $EMIM^+$ and their ratios measured using pulsed field gradient (PFG)-NMR.

D ($\times 10^{-10}$ m^2/s)	KCl + EMIMCl	$PbCl_2$ + KCl + EMIMCl
D(H_2O)	18.91	18.86
D($EMIM^+$)	9.19	9.00
D(H_2O)/D($EMIM^+$)	2.06	2.09

Table S4. Calculated HOMO and LUMO energies and HOMO-LUMO gaps of gas-phase $PbCl_3^-$ and $Pb_2Cl_5^-$ clusters and their complexes with EMIMCl as a function of EMIMCl molecules.

Clusters	LUMO (eV)	HOMO (eV)	HOMO-LUMO Gap (eV)
$PbCl_3^-$	1.8	-2.3	4.1
$[PbCl_3 + EMIMCl]^-$	1.0	-1.7	2.6
$[PbCl_3 + 2EMIMCl]^-$	0.8	-2.4	3.3
$[PbCl_3 + 3EMIMCl]^-$	0.6	-2.8	3.3
$[PbCl_3 + 4EMIMCl]^-$	0.5	-2.9	3.5
$Pb_2Cl_5^-$	0.8	-3.3	4.0
$[Pb_2Cl_5 + EMIMCl]^-$	0.9	-3.4	4.3
$[Pb_2Cl_5 + 2EMIMCl]^-$	0.4	-2.9	3.3

Table S5. Calculated HOMO and LUMO energies and HOMO-LUMO gaps of solution-phase $PbCl_2$, $PbCl_3^-$, $PbCl_4^{2-}$ and $PbCl_5^{3-}$ clusters and their complexes with EMIMCl as a function of EMIMCl molecules.

Clusters	LUMO (eV)	HOMO (eV)	HOMO-LUMO Gap (eV)
$PbCl_2$	-2.7	-6.7	4.0
[$PbCl_2$ + 1EMIMCl]	-2.7	-6.7	4.0
[$PbCl_2$ + 2EMIMCl]	-2.6	-6.5	3.9
[$PbCl_2$ + 3EMIMCl]	-2.7	-6.6	3.9
[$PbCl_2$ + 4EMIMCl]	-2.7	-6.5	3.8
$PbCl_3^-$	-1.1	-6.0	4.9
$[PbCl_3 + 1EMIMCl]^-$	-1.7	-6.1	4.3
$[PbCl_3 + 2EMIMCl]^-$	-1.5	-6.1	4.5
$[PbCl_3 + 3EMIMCl]^-$	-1.7	-6.3	4.5
$[PbCl_3 + 4EMIMCl]^-$	-1.8	-6.4	4.5
$PbCl_4^{2-}$	-0.9	-5.1	4.2
$[PbCl_4 + 1EMIMCl]^{2-}$	-1.4	-5.3	3.9
$[PbCl_4 + 2EMIMCl]^{2-}$	-1.8	-5.4	3.7
$[PbCl_4 + 3EMIMCl]^{2-}$	-1.6	-5.5	3.9
$[PbCl_4 + 4EMIMCl]^{2-}$	-1.6	-5.6	3.9
$PbCl_5^{3-}$	-0.8	-4.8	4.1
$[PbCl_5 + 1EMIMCl]^{3-}$	-1.2	-4.9	3.8
$[PbCl_5 + 2EMIMCl]^{3-}$	-1.4	-5.0	3.6
$[PbCl_5 + 3EMIMCl]^{3-}$	-1.5	-5.1	3.6
$[PbCl_5 + 4EMIMCl]^{3-}$	-1.5	-5.3	3.7